NCEP NOTES

Implementation in the NCEP GFS of a Hybrid Eddy-Diffusivity Mass-Flux (EDMF) Boundary Layer Parameterization with Dissipative Heating and Modified Stable Boundary Layer Mixing

JONGIL HAN

Systems Research Group, Inc., Environmental Prediction Center, National Centers for Environmental Prediction, College Park, Maryland

MARCIN L. WITEK AND JOAO TEIXEIRA

Jet Propulsion Laboratory, California Institute of Technology, Pasadena, California

RUIYU SUN AND HUA-LU PAN

I.M. Systems Group, Inc., Environmental Prediction Center, National Centers for Environmental Prediction, College Park, Maryland

JENNIFER K. FLETCHER AND CHRISTOPHER S. BRETHERTON

Department of Atmospheric Sciences, University of Washington, Seattle, Washington

(Manuscript received 28 April 2015, in final form 12 June 2015)

ABSTRACT

The current operational eddy-diffusivity countergradient (EDCG) planetary boundary layer (PBL) scheme in the NCEP Global Forecast System (GFS) tends to underestimate the PBL growth in the convective boundary layer (CBL). To improve CBL growth, an eddy-diffusivity mass-flux (EDMF) PBL scheme is developed, where the nonlocal transport by large turbulent eddies is represented by a mass-flux (MF) scheme and the local transport by small eddies is represented by an eddy-diffusivity (ED) scheme. For the vertical momentum mixing, the MF scheme is modified to include the effect of the updraft-induced pressure gradient force. While the EDMF scheme displays better CBL growth than the EDCG scheme, it tends to overproduce the amount of low clouds and degrades wind vector forecasts over the tropical ocean where strongly unstable PBLs are rarely found. In order not to degrade the forecast skill in the tropics, a hybrid scheme is developed, where the EDMF scheme is applied only for the strongly unstable PBL, while the EDCG scheme is used for the weakly unstable PBL. Along with the hybrid EDMF scheme, the heating by turbulent kinetic energy (TKE) dissipation is parameterized to reduce an energy imbalance in the GFS. To enhance a too weak vertical turbulent mixing for weakly and moderately stable conditions, the current local scheme in the stable boundary layer (SBL) is modified to use an eddy-diffusivity profile method. The hybrid EDMF PBL scheme with TKE dissipative heating and modified SBL mixing led to significant improvements in some key medium-range weather forecast metrics and was operationally implemented into the NCEP GFS in January 2015.

1. Introduction

The planetary boundary layer (PBL) scheme in the National Centers for Environmental Prediction's (NCEP) Global Forecast System (GFS) adopts an eddy-diffusivity countergradient (EDCG) mixing approach (Deardorff 1966; Troen and Mahrt 1986; Hong and Pan 1996; Han and Pan 2011) to take into account nonlocal transport by strong updrafts in the daytime convective boundary layer (CBL). Although the GFS EDCG PBL scheme provides a realistic CBL development projection despite its simplicity, it has been found to underpredict the daytime CBL growth (Noh et al. 2003; Siebesma et al. 2007). Siebesma et al. (2007) show that the underestimation of

Corresponding author address: Jongil Han, NCEP/EMC, 5830 University Research Ct., College Park, MD 20740.
E-mail: jongil.han@noaa.gov

DOI: 10.1175/WAF-D-15-0053.1

the CBL growth by the EDCG approach is due to too weak entrainment flux at the CBL top, which is caused by a positive countergradient (CG) term over the entire CBL.

To have better PBL growth in the CBL, an eddy-diffusivity mass-flux (EDMF) PBL scheme is developed based on Siebesma and Teixeira (2000), Soares et al. (2004), and Siebesma et al. (2007). In the EDMF approach, the nonlocal subgrid transport due to the strong updrafts is taken into account by a mass-flux (MF) scheme and the remaining transport by smaller eddies is handled by an eddy-diffusivity (ED) scheme. The nonlocal momentum transport is also developed with the MF approach, which is missing in the original Siebesma et al. (2007) EDMF scheme.

PBL models based on the EDMF concept are being more widely used in weather and climate prediction models. For example, Köhler et al. (2011) implemented an EDMF scheme in the European Centre for Medium-Range Weather Forecasts (ECMWF) model. Hourdin et al. (2013) presented an implementation of the thermal plume model (Rio and Hourdin 2008), an EDMF-type scheme, in the Laboratoire de Météorologie Dynamique model (LMDZ; with Z standing for the model zoom capacity). Recently, Sušelj et al. (2014) developed a unified boundary layer and shallow convection parameterization based on a stochastic EDMF approach and implemented the scheme in the Navy Global Environmental Model (NAVGEM).

Initial tests indicate that while the EDMF scheme predicts the CBL growth well, it tends to have too much vertical mixing in wind and moisture over the tropics, giving rise to unrealistically large low cloud amounts as well as largely degraded wind vector forecasts in the tropics. This led to the development of a hybrid EDMF PBL scheme, which will be discussed in detail later. On the other hand, heating by the dissipation of turbulent kinetic energy (TKE) is usually neglected in numerical weather and climate prediction models because of its small magnitude. Bister and Emanuel (1998) first recognized that the viscous dissipation of TKE can be a significant source of heat in hurricanes. Afterward, many studies (e.g., Zhang and Altshuler 1999; Jin et al. 2007) have shown that the inclusion of TKE dissipative heating increases the surface maximum wind by about 10%–30% in hurricane forecasts. In this study, the TKE dissipative heating is parameterized and included in the hybrid EDMF PBL scheme. In addition, the current local scheme in the stable boundary layer (SBL) is modified to improve vertical turbulent mixing for weakly and moderately stable conditions.

The implementation procedure associated with model physics changes in the NCEP operational numerical weather prediction (NWP) system is as follows: 1) identify model forecast biases or problems (e.g., the present study was motivated by the problem of underestimated PBL growth with the current EDCG PBL scheme in strongly unstable conditions), 2) reduce the bias by updating the model physics with more realistic parameterizations (e.g., develop the EDMF PBL scheme to have better PBL growth in strongly unstable conditions), 3) test the updated scheme in the operational mode, and, finally, 4) implement the scheme into the operational model if the forecast skill is improved or at least neutral, otherwise, reject the scheme even though it may be more realistic in many respects. A better scheme is not always guaranteed to produce a statistically improved forecast skill due to adverse interactions among model physics parameterizations and with the dynamics. While more specific case studies are helpful for a detailed investigation on how and why a particular scheme improves the forecast, our study focuses on statistical forecast skill improvement over the longer term, which is the main concern in operational NWP centers.

Details of the parameterizations and modifications are described in section 2. In section 3, we evaluate the impacts of the new scheme on medium-range forecasts. Finally, in section 4 we summarize our study.

2. Development of hybrid EDMF PBL parameterization with dissipative heating and modified SBL mixing

The NCEP GFS is a global spectral model for weather and climate prediction. The radiation parameterization uses the Rapid Radiative Transfer Model (RRTM) adapted from Atmospheric and Environmental Research (AER), Inc. (e.g., Mlawer et al. 1997; Iacono et al. 2000; Clough et al. 2005). The orographic gravity wave drag parameterization is adopted from Kim and Arakawa (1995). The cloud condensate is a prognostic quantity with a simple cloud microphysics parameterization (Zhao and Carr 1997; Sundqvist et al. 1989; Moorthi et al. 2001). The fractional cloud cover used for radiation purposes is diagnostically determined by the predicted cloud condensate, following the study by Xu and Randall (1996). The Noah land surface model (Ek et al. 2003) is used and the surface layer similarity formulations are based on Long (1986, 1989).

Recently, parameterizations for deep and shallow cumulus convection and vertical turbulent mixing have been greatly revised (Han and Pan 2011). The shallow cumulus convection scheme now employs a mass-flux

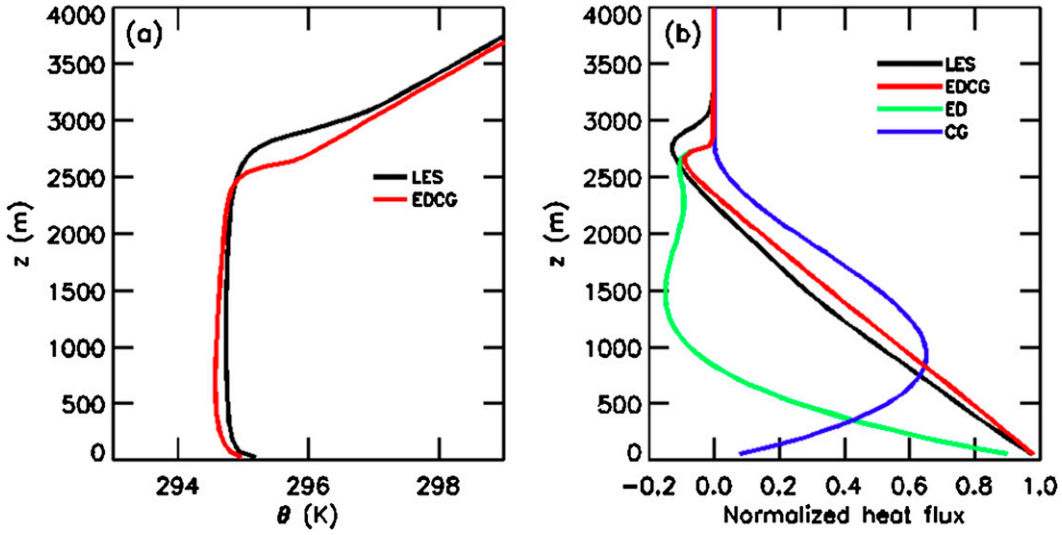

FIG. 1. SCM results with the EDCG scheme compared with LES results after an 8-h simulation. Vertical profiles of (a) potential temperature and (b) total turbulent heat fluxes normalized by surface heat flux with the breakdown of heat flux of the EDCG scheme into ED and CG contributions.

parameterization replacing the old turbulent diffusion–based approach. For deep cumulus convection, the scheme was revised to make convection stronger and deeper to suppress excessive grid-scale precipitation. The PBL model was revised to enhance turbulent diffusion in stratocumulus regions. In this study, we further update the PBL model using the EDMF approach.

a. Hybrid EDMF parameterization for the CBL

In the GFS EDCG PBL scheme, the vertical turbulent flux of a field ϕ for the dry CBL is given by

$$\overline{w'\phi'} = -K\left(\frac{\partial\overline{\phi}}{\partial z} - \gamma\right), \tag{1}$$

where overbars indicate a spatial average, primes represent turbulent fluctuations, K is the turbulent eddy diffusivity, and γ is the nonlocal CG mixing term due to large nonlocal convective eddies and applied only to the temperature field. The formulation for γ is given by (Troen and Mahrt 1986)

$$\gamma = b\,\frac{(\overline{w'\phi'})_0}{w_s h}, \tag{2}$$

where $(\overline{w'\phi'})_0$ is the surface turbulent flux of variable ϕ, w_s is a velocity scale, h is the PBL height, and b is a constant. For the turbulent heat flux, therefore, the CG term in Eq. (1), $K\gamma$, is always positive since the surface heat flux in the CBL is positive. The scheme adopts an eddy-diffusivity profile K derived by Troen and Mahrt (1986) as

$$K = \mathrm{Pr}^{-1}\kappa w_s z\left(1 - \frac{z}{h}\right)^p, \tag{3}$$

where $\kappa = 0.4$ is the von Kármán constant and Pr is the Prandtl number. The exponent $p = 2$ is used.

Figure 1 compares the vertical profiles of potential temperature and turbulent heat flux simulated after 8 h by a large-eddy simulation (LES) with the GFS single-column model (SCM) result using the EDCG scheme. For the simulations, an initial potential temperature profile $\theta = 288\,\mathrm{K} + (3\,\mathrm{K\,km^{-1}})z$ is used and a constant surface buoyancy flux ($8 \times 10^{-3}\,\mathrm{m^2\,s^{-3}}$) is specified. The LES model used here is version 6 of the System for Atmospheric Modeling (SAM; Khairoutdinov and Randall 2003). The vertical grid size for the SCM is 50 m, which is the same as that in the LES. Figure 1b clearly shows that the underprediction of the CBL growth seen in Fig. 1a is caused by a too weak entrainment flux at the CBL top due to the positive CG term over the entire CBL, as also shown by the Siebesma et al. (2007) study. Note that the CBL growth is influenced by both the heat flux at the surface and the entrainment flux at the top.

In the EDMF scheme (Siebesma et al. 2007), the nonlocal countergradient mixing term in Eq. (1) is replaced by a mass-flux approach; that is,

$$\overline{w'\phi'} = -K\,\frac{\partial\overline{\phi}}{\partial z} + M(\phi_u - \overline{\phi}), \tag{4}$$

where the subscript u refers to the updraft properties and M denotes the updraft mass flux. The mass flux is given by

$$M = a_u(w_u - \overline{w}) \approx a_u w_u, \tag{5}$$

where a_u is a small, fixed updraft fractional area that contains the strongest upward vertical velocities. The updraft velocity w_u is computed using (Soares et al. 2004)

$$\frac{\partial w_u^2}{\partial z} = -b_1 \varepsilon w_u^2 + b_2 B, \tag{6}$$

with the buoyancy $B = g(\theta_{v,u} - \overline{\theta}_v)/\overline{\theta}_v$ as a source term (where θ_v is the virtual potential temperature and g is the gravity). In Eq. (6), ε is the lateral entrainment rate, described below. The optimal values of the coefficients, b_1 and b_2, will be discussed later. Recently, de Roode et al. (2012) found that the dominant sink term in the updraft velocity budget is not the entrainment rate for updraft velocity, but the pressure gradient term. However, they show that the pressure gradient term can be related to the entrainment rate for thermodynamic quantities [i.e., the first term on the right-hand side of Eq. (6)] or the buoyancy term. This aspect warrants further study.

The updraft properties are obtained using a simple entraining plume model:

$$\frac{\partial \phi_u}{\partial z} = -\varepsilon(\phi_u - \overline{\phi}). \tag{7}$$

According to the LES results (Siebesma et al. 2007), the entrainment rate, related to the lateral mixing of the updraft with the environment, is given by

$$\varepsilon = c_\varepsilon \left[\frac{1}{z + \Delta z} + \frac{1}{(h - z) + \Delta z} \right], \tag{8}$$

where Δz represents the vertical grid size and c_ε is an empirical coefficient. The addition of Δz helps to avoid divergence when z approaches zero or h is close to a model level. Other entrainment rate formulations have been suggested in the literature (e.g., Neggers et al. 2002, 2009; Rio and Hourdin 2008; Köhler et al. 2011; Witek et al. 2011). Witek et al. (2011) compared different ε parameterizations for various dry convection scenarios and showed that they largely agree with each other and lead to similar results.

Following Siebesma et al. (2007), the buoyancy at the lowest level is given by

$$\theta_{v,u}(z_1) - \overline{\theta}_v(z_1) = \alpha \frac{Q_s}{\sigma_w(z_1)}, \tag{9}$$

where Q_s is the surface sensible heat flux and the coefficient $\alpha = 1.0$. The standard deviation of the vertical turbulent velocity at the lowest model level, $\sigma_w(z_1)$, is given by

$$\sigma_w = 1.3\left(u_*^3 + 0.6 w_*^3 \frac{z_1}{h}\right)^{1/3} \left(1 - \frac{z_1}{h}\right)^{1/2}, \tag{10}$$

where u_* and w_* are the friction velocity and the CBL velocity scale, respectively. Above the lowest model level, $\theta_{v,u}$ is obtained using Eq. (7).

Determination of the PBL height is of crucial importance for the PBL growth in the EDCG scheme because it imposes the vertical extent of the diffusivity profile in Eq. (3). Following Troen and Mahrt (1986), h is given by

$$h = \mathrm{Rb}_{\mathrm{cr}} \frac{\theta_{va} |U(h)|^2}{g[\theta_v(h) - \theta_s]}. \tag{11}$$

Here, $\mathrm{Rb}_{\mathrm{cr}}$ is the critical bulk Richardson number (currently, $\mathrm{Rb}_{\mathrm{cr}} = 0.25$), $U(h)$ is the horizontal wind speed at $z = h$, θ_{va} is the virtual potential temperature at the lowest model level, $\theta_v(h)$ is the virtual potential temperature at $z = h$, and θ_s is the temperature scale near the surface defined as

$$\theta_s = \theta_{va} + \theta_T. \tag{12}$$

In Eq. (12), θ_T is a thermal excess proportional to the surface sensible heat flux and plays an important role in the PBL growth. Note that in the EDCG model h represents the height of zero heat flux, that is, $(\overline{w'\theta'})_{z=h} = 0$, and, thus, h is located above the minimum heat flux. As a consequence, the entrainment fluxes just below h are implicitly determined to be proportional to h. As mentioned above, these negative entrainment fluxes are largely reduced by the positive CG term, resulting in an undergrowth of the PBL.

In the EDMF scheme, two different PBL heights are used. The h in Eq. (3) is determined from Eq. (11) but without the thermal excess in Eq. (12). For the MF part in Eq. (4), h is defined as the height of $w_u = 0$ from Eq. (6), so that the updraft overshoots into the upper stable layer and produces negative entrainment fluxes in the upper PBL. For diagnostic purposes, h is defined as Eq. (11) but without the thermal excess in Eq. (12).

A mass-flux mixing for momentum is also included but with the effect of the updraft-induced pressure gradient force (Han and Pan 2006), which weakens the momentum exchange due to the vertical mass flux. This is similar to the nonlocal momentum mixing suggested by Frech and Mahrt (1995), Brown and Grant (1997), and Noh et al. (2003) in that the nonlocal mixing for momentum is much weaker than that for heat and moisture. It is also consistent with the fact that in the CBL, the turbulent eddy diffusivity for momentum is much smaller than that for heat and moisture. Following Han and Pan's study, the updraft property for momentum is written as

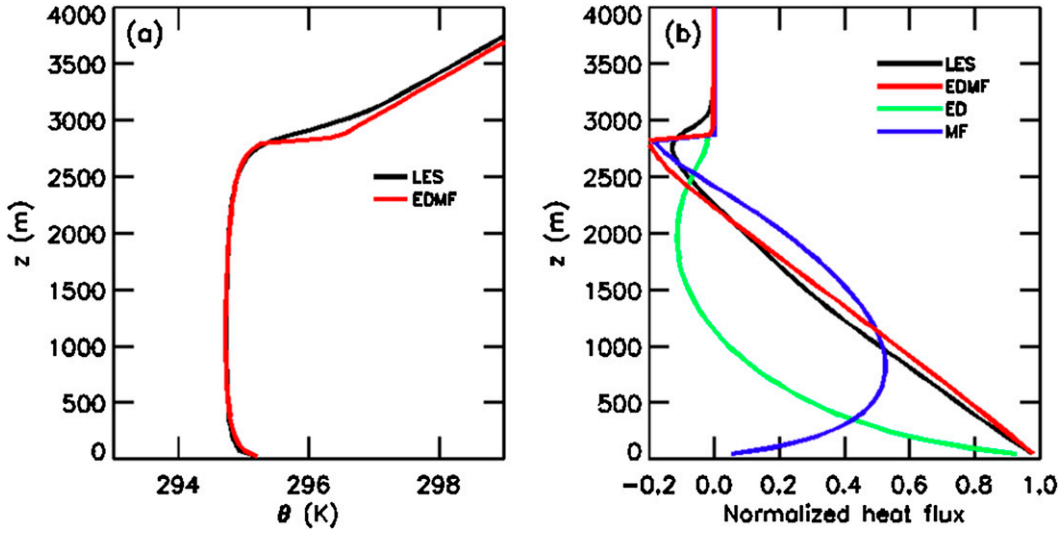

FIG. 2. As in Fig. 1, but for SCM results with the EDMF scheme.

$$\frac{\partial \mathbf{V}_u}{\partial z} = -\varepsilon(\mathbf{V}_u - \overline{\mathbf{V}}) + d_1 \frac{\partial \overline{\mathbf{V}}}{\partial z}, \qquad (13)$$

where $\mathbf{V}$ is the horizontal wind vector and d_1 an empirical constant representing the effect of the updraft-induced pressure gradient force, given as $d_1 = 0.55$ from the Zhang and Wu (2003) cloud-resolving model results. Since the constant d_1 is derived from cumulus convection, a detailed study using LES for the effect of the updraft-induced pressure gradient force in the CBL would be worthwhile.

The tunable coefficients of this implementation, a_u, b_1, b_2, and c_ε, are somewhat sensitive to the vertical grid resolution. The optimal coefficient values used for the SCM, for which the vertical grid size is 50 m, are $a_u = 0.1$, $b_1 = 1.8$, $b_2 = 4.0$, and $c_\varepsilon = 0.37$. These values are comparable to those used in Soares et al. (2004) and Siebesma et al. (2007). In Soares et al. (2004), for example, $a_u = 0.1$, $b_1 = 2.0$, $b_2 = 4.0$, and $c_\varepsilon = 0.5$, whereas in Siebesma et al. (2007), $a_u = 0.12$, $b_1 = 1.43$, $b_2 = 2.86$, and $c_\varepsilon = 0.4$. Figure 2a displays the GFS-SCM result using the EDMF scheme and shows that the EDMF scheme predicts the CBL growth well compared to the LES. As shown in Fig. 2b, the better CBL growth in the EDMF scheme compared to the EDCG scheme (Fig. 1b) is mainly due to a larger entrainment flux induced by the mass-flux term. However, when we use the operational GFS vertical grid spacing, which is ~200 m at about 1-km level above the surface, the CBL growth with the EDMF scheme tends to be overpredicted, as seen in Fig. 3. Therefore, the coefficients were optimized again for better CBL growth at the operational GFS resolution as $a_u = 0.08$, $b_1 = 1.8$, $b_2 = 3.5$, and $c_\varepsilon = 0.38$ (Fig. 3). Although not shown, one of the reasons for the sensitivity to the vertical resolution is the dependency of the entrainment rate [Eq. (8)] on the vertical grid size (Δz). Thus, entrainment parameterizations that are not directly related to the vertical grid size (e.g., Köhler et al. 2011; Witek et al. 2011) will be investigated in future studies.

To investigate the impact of the new EDMF PBL scheme, medium-range forecasts have been conducted

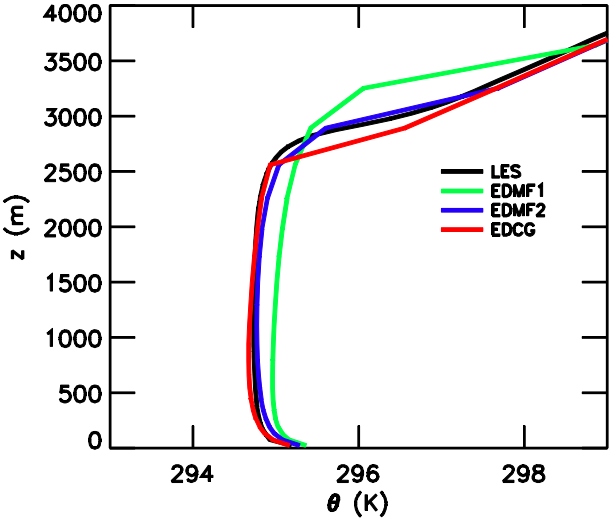

FIG. 3. Vertical profiles of potential temperature from the SCM results with the current operational GFS vertical resolution compared with LES results after an 8-h simulation. The green line (EDMF1) represents the EDMF scheme result with the same tunable parameters as those used in high-resolution SCM tests (i.e., $a_1 = 0.1$, $b_1 = 1.8$, $b_2 = 4.0$, and $c_e = 0.37$), the blue line (EDMF2) shows the EDMF scheme result with parameters optimized for the operational GFS vertical resolution (i.e., $a_1 = 0.08$, $b_1 = 1.8$, $b_2 = 3.5$, and $c_e = 0.38$), and the red line shows the EDCG scheme result.

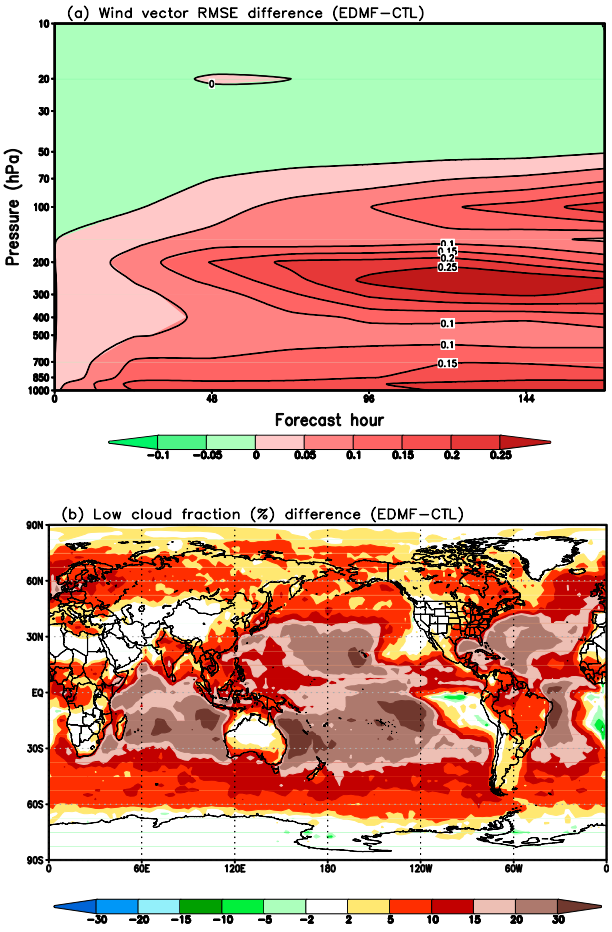

FIG. 4. Mean differences between EDMF scheme and control forecasts of (a) wind vector RMSE over the tropics (30°S–30°N) and (b) low cloud fraction. The forecast period for the mean difference calculation is from 7 Jul to 31 Oct 2012, and the low cloud fraction is the average of 102, 108, 114, and 120 forecast hours.

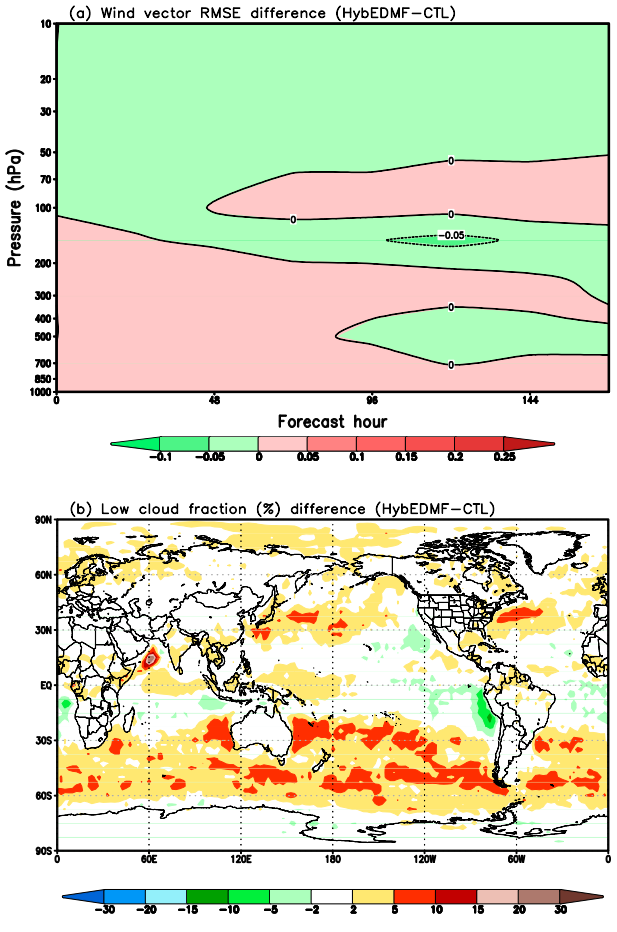

FIG. 5. As in Fig. 4, but for the hybrid EDMF scheme.

with initial conditions from the operational GFS analysis data. Initial tests indicated that the EDMF scheme improved the forecast skill in the 500-mb height anomaly correlation over the midlatitudes and in precipitation (especially light rain) over the continental United States. However, it degraded the tropical wind vector forecast and also increased low cloud amounts too much over the tropics, as shown in Fig. 4. In order not to degrade the forecast skill over the tropics, a hybrid EDMF scheme is developed, where the EDMF scheme is applied only for the strongly unstable PBL (i.e., CBL) while the EDCG scheme is retained for the weakly unstable PBL. Note that unlike for strongly unstable conditions, the EDCG scheme does not underestimate the PBL growth for weakly unstable conditions (Noh et al. 2003). A detailed investigation on why using this version of EDMF for weakly unstable conditions may slightly degrade forecast skill in the GFS will be performed in a future study. The z/L [L is the Monin–Obukhov length, defined as $L = -u_*^3\theta_{va}/\kappa g(\overline{w'\theta_v'})_s$, where $(\overline{w'\theta_v'})_s$ is the surface buoyancy flux] is used as the stability criterion for the PBL [currently, strongly unstable (convective) PBL for $z/L < -0.5$ and weakly and moderately unstable PBL for $0 > z/L > -0.5$ (Sorbjan 1989)]. Since the tropics are comprised mainly of oceans where a strongly unstable PBL is rarely found, the EDCG scheme would mostly be used over the tropics in the hybrid scheme. As a result, the hybrid scheme not only significantly reduces the tropical wind vector RMSE but also prohibits too much of an increase of low clouds over the tropics, as shown in Fig. 5.

b. *Dissipative heating parameterization*

Viscous dissipation of TKE can be a significant source of heat especially in strong wind conditions such as hurricanes, but its effect is not taken into account in the current operational GFS. On the other hand, excluding the dissipative heating can cause a significant energy imbalance in an atmospheric model (Fiedler 2000).

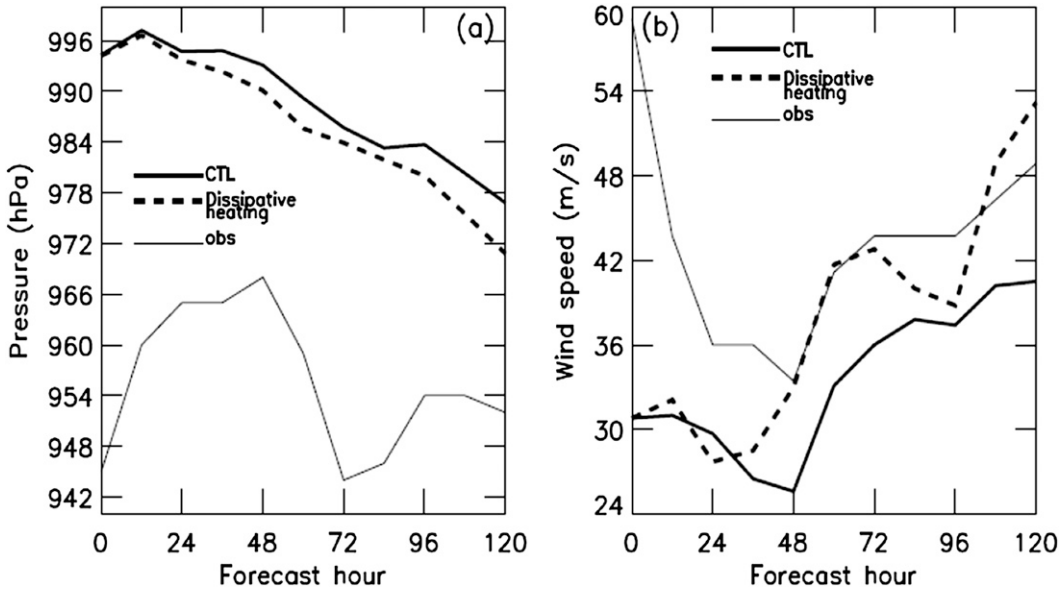

FIG. 6. Time evolution of (a) min central mean sea level pressure and (b) max 10-m wind speed with (dashed line) and without (solid line) TKE dissipative heating for Hurricane Ike (2008). The observed intensities from the best-track data are displayed as light solid lines.

The TKE dissipative heating can be expressed as (Jin et al. 2007)

$$c_p \left.\frac{\partial \overline{T}}{\partial t}\right|_{\text{diss}} \approx D, \tag{14}$$

where T is the temperature, t is the time, and D is the dissipation rate of TKE and can be estimated from the TKE budget equation. Assuming that buoyancy and shear production of TKE are balanced by TKE dissipation, the TKE budget equation can be simplified as

$$D \approx \frac{g}{\overline{\theta}_v}\overline{w'\theta'_v} - \overline{u'w'}\frac{\partial \overline{u}}{\partial z}, \tag{15}$$

where u and w represent the horizontal and vertical velocities, respectively, and the primes indicate turbulent fluctuations while the overbars represent a spatial average. Using the surface layer similarity theory, the mean TKE dissipation over the depth of the surface layer z_1 can be written as

$$\overline{D} \approx \frac{g}{\overline{\theta}_v}(\overline{w'\theta'_v})_s + \frac{u_*^2 \overline{u}_1}{z_1}. \tag{16}$$

Above the surface layer, using a downgradient turbulent transport assumption with eddy diffusivity, the mean TKE dissipation can be written as

$$\overline{D} \approx -\frac{g}{\overline{\theta}_v} K \frac{\partial \overline{\theta}_v}{\partial z} + \mathrm{Pr} K \left(\frac{\partial \overline{u}}{\partial z}\right)^2. \tag{17}$$

The TKE dissipation is dominant generally in the surface layer because of the strong shear production of TKE. Although not shown, the mean temperature increase in the surface layer due to dissipative heating is typically less than 0.5 K, except for strong wind cases such as hurricanes.

Figure 6 displays the impact of TKE dissipative heating on a hurricane forecast. It shows that the hurricane intensity (e.g., maximum 10-m wind speed) can be significantly increased in the GFS forecast with TKE dissipative heating, consistent with the studies such as those of Zhang and Altshuler (1999) and Jin et al. (2007). Note that the hurricane intensity in the GFS is generally much weaker than the observations, which is mainly due to coarse resolution and missing physics such as the TKE dissipative heating in the present study. On the other hand, the energy balance test results with TKE dissipative heating (Table 1) show that a large atmospheric energy loss (about 4–5 W m^{-2}) found in the GFS atmosphere–ocean coupled run can be largely reduced with the inclusion of TKE dissipative heating, leading to an improved global energy balance.

c. *Modification in the SBL vertical mixing scheme*

Before July 2010, a K-profile method [e.g., Eq. (3)] was used in the GFS for the vertical turbulent mixing in the stable boundary layer, and was reported to show too strong turbulent mixing and consequently a too deep SBL (Cuxart et al. 2006). In the July 2010 upgrade (Han and Pan 2011), therefore, a local scheme is adopted for

TABLE 1. Energy balance test results from the GFS atmosphere–ocean coupled (1 yr) run with (EXP) and without (CTL) TKE dissipative heating. TOA represents the mean energy budget at the top of the atmosphere, SFC is the mean energy budget at the surface, and difference is the mean energy budget at the TOA minus the SFC [indicating mean energy loss (positive) or gain (negative) in the model atmosphere].

	TOA ($W\,m^{-2}$)	SFC ($W\,m^{-2}$)	Difference ($W\,m^{-2}$)
CTL	9.9	5.3	4.6
EXP	1.5	0.8	0.7

the SBL to reduce vertical turbulent mixing, which is given as

$$K = l^2 f(\mathrm{Ri}) \left| \frac{\partial \overline{u}}{\partial z} \right|, \tag{18}$$

where l is the mixing length and $f(\mathrm{Ri})$ is the stability function, where Ri is the local gradient Richardson number. However, Hong (2010) reports that the local scheme, Eq. (18), tends to present cold and moist biases in the lower troposphere during the nighttime because of too weak vertical turbulent mixing. An internal briefing at NCEP also indicates a cold bias near the surface especially in weakly stable conditions, which is attributed to the local scheme [Eq. (18)]. Therefore, we modify the scheme so that the local scheme [i.e., Eq. (18)] is used for the strongly stable condition where turbulence is often sporadic, but the K-profile method [i.e., Eq. (3)] is adopted for the weakly and moderately stable conditions where turbulence is continuous. The z/L is again used as the stability criterion [currently, strongly stable for $z/L > 0.2$ and weakly and moderately stable for $0 < z/L < 0.2$ (Sorbjan 1989)].

On the other hand, the K-profile method requires the determination of PBL height, which is given by Eq. (11). For the SBL, θ_s in Eq. (12) is the surface potential temperature without the thermal excess. From the analysis of three field program datasets, Vickers and Mahrt (2004) find that for the SBL the use of $\mathrm{Rb_{cr}}$ varying with the surface Rossby number in Eq. (11) gives the best estimation of the SBL height. We adopt Vickers and Mahrt's Rossby number–dependent critical bulk Richardson number, which is written as

$$\mathrm{Rb_{cr}} = 0.16(10^{-7} R_0)^{-0.18}, \tag{19}$$

where R_0 is the surface Rossby number, which is given as

$$R_0 = \frac{U_{10}}{f_0 z_0}, \tag{20}$$

where U_{10} is the wind speed at 10 m above the ground surface, f_0 is the Coriolis parameter, and z_0 is the surface roughness length. To avoid too much variation, we restrict $\mathrm{Rb_{cr}}$ to vary within the range of ~0.15–0.35. As expected (not shown), the modified scheme for the SBL significantly reduces the cold bias near the surface by virtue of the enhanced vertical turbulent mixing. Hong (2010) also adopted Vickers and Mahrt's Rossby number–dependent critical bulk Richardson number, which gave a better simulation of the East Asian summer monsoon.

3. Medium-range forecast results

To assess the impacts of the new scheme (i.e., the hybrid EDMF PBL scheme with TKE dissipative heating and modification in the SBL) on forecast skill, 7-day forecasts for the period from 1 July to 31 October 2012 were conducted. The initial forecast time was at 0000 UTC for each day. The GFS used in this test has 64 vertical sigma-pressure hybrid layers and T574 (about 35 km) horizontal resolution. Since the forecasts were performed with no data assimilation, the analysis data from the operational GFS were used as the initial conditions. Although tests with data assimilation would be desirable, they not only cost too much in computing time but the study of Park and Hong (2013) seems to indicate that initial conditions are not always essential when evaluating the impact of model physics changes.

A comparison of anomaly correlations for the 500-hPa height, which illustrates how well synoptic-scale systems are represented around the globe, is shown in Fig. 7 as a function of forecast length. In both the Northern (20°–80°N) and Southern (20°–80°S) Hemispheres, the new scheme displays better anomaly correlations than does the control forecast. Although the improvement is somewhat small, it is still significant.

Comparisons of equitable threat and bias scores (Gandin and Murphy 1992) for the 12–36-h precipitation forecasts over the continental United States are shown in Fig. 8. Compared to the control forecasts, the equitable threat score (Fig. 8a) is slightly better for light rain but slightly worse for heavy rain. For the bias (Fig. 8b), the new scheme is wetter than the control for heavy rain. However, the forecast skill differences for both equitable threat and bias scores are not significant. Although not shown, the forecast skill differences for the 36–60- and 60–84-h precipitation forecasts were very similar to those in the 12–36-h precipitation forecasts.

The performance of the new scheme for hurricane forecasts is shown in Fig. 9 in terms of hurricane track and intensity errors, and shows a mixed signal. Compared to the control track forecast (Figs. 9a,b), the new scheme shows a smaller error at 120 forecast hours for 2012 Atlantic hurricanes, but it displays a larger error at

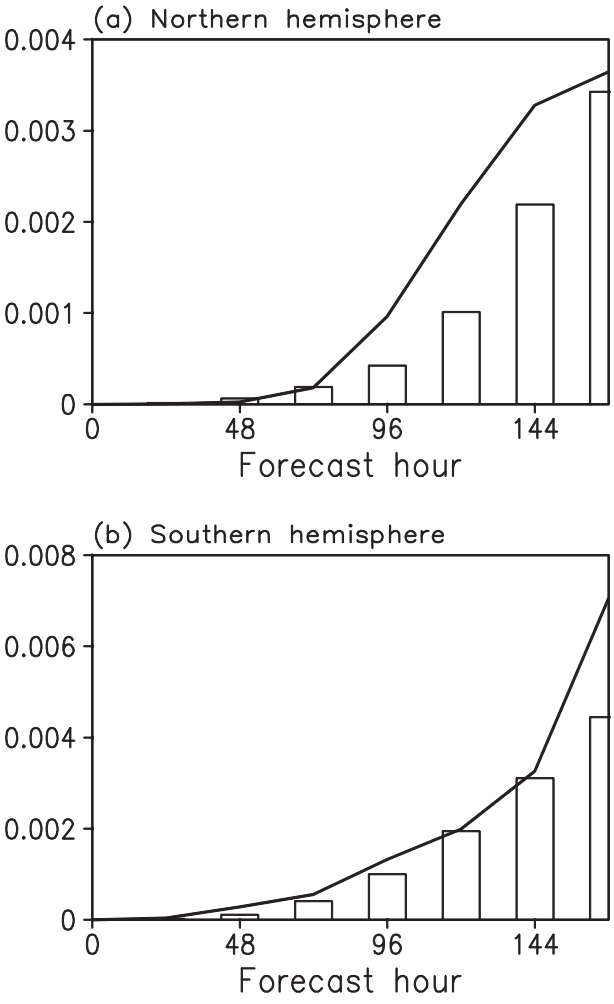

FIG. 7. Mean difference in anomaly correlations of 500-hPa height for the forecasts with the new scheme with respect to the control forecasts in the (a) Northern Hemisphere (20°–80°N) and (b) Southern Hemisphere (20°–80°S) from 7 Jul to 31 Oct 2012. The differences outside the rectangle bars are statistically significant at the 95% confidence level.

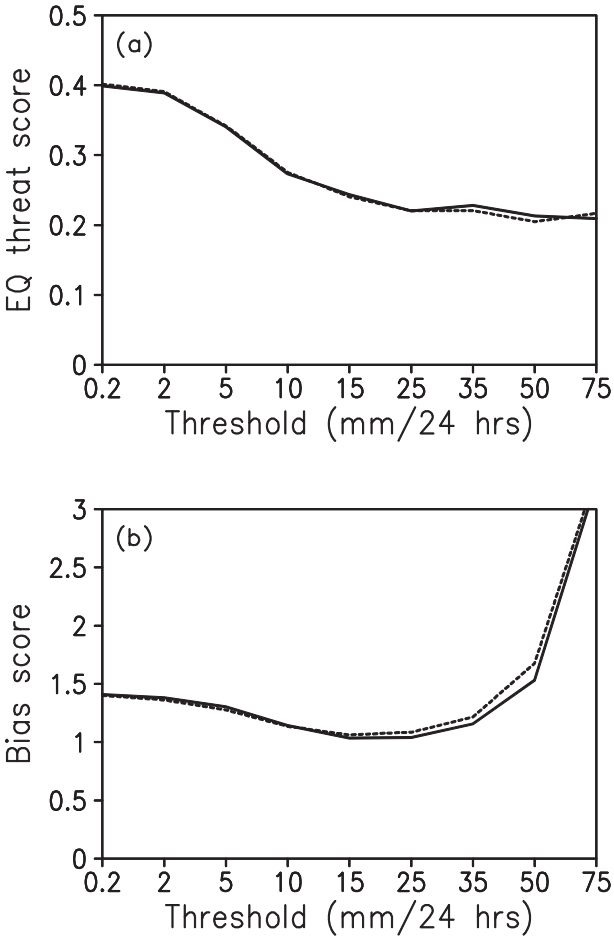

FIG. 8. Mean (a) equitable threat score and (b) bias score for 12–36-h precipitation forecasts over the continental United States for the control forecasts (solid line) and forecasts with the new scheme (dashed line) from 7 Jul to 31 Oct 2012.

72 and 96 forecast hours for 2012 eastern Pacific hurricanes. For the intensity forecast (Figs. 9c,d), the new scheme shows a smaller error than the control for 2012 eastern Pacific hurricanes for most forecast times, but for 2012 Atlantic hurricanes it displays a slightly larger error than the control, especially at forecast times of less than 24 h. In general, the error differences between the new scheme and the control are quite small for both hurricane track and intensity forecasts.

4. Summary and conclusions

The current operational eddy-diffusivity countergradient (EDCG) planetary boundary layer (PBL) scheme in the NCEP GFS underestimates PBL growth in the convective boundary layer (CBL) because of a positive countergradient (CG) mixing term in the entrainment zone. To improve the PBL growth in the CBL, an eddy-diffusivity mass-flux (EDMF) PBL scheme is developed for the GFS, where the constant CG mixing term is replaced by a mass-flux (MF) scheme. For the vertical momentum mixing, the MF scheme is further modified to include the effect of the updraft-induced pressure gradient force, which weakens the vertical momentum exchange.

The EDMF scheme predicts the CBL growth well compared to large-eddy simulation results. Over the tropics, however, the EDMF scheme tends to overproduce the amounts of low clouds and degrades the wind vector forecasts. Note that the tropics are mostly composed of oceans where a strongly unstable PBL is rarely found. In order not to degrade the forecast skill in the tropics a hybrid scheme is developed, where the

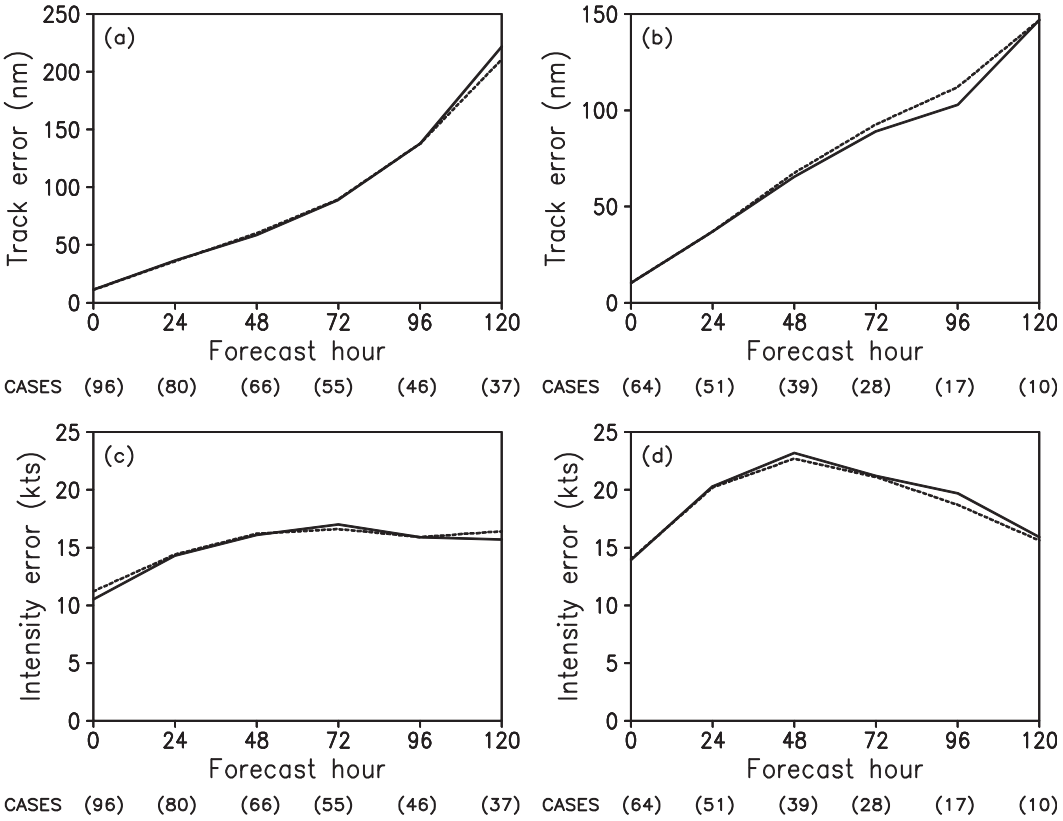

FIG. 9. As in Fig. 8, but for mean hurricane (a),(b) track and (c),(d) intensity errors for the (left) Atlantic and (right) eastern Pacific Ocean regions.

EDMF scheme is applied only for the strongly unstable PBL (i.e., CBL), while the EDCG scheme is used for the weakly unstable PBL. As a result, the EDCG scheme is mostly called over the tropics in the hybrid scheme.

To improve a significant energy imbalance in the coupled GFS, the heating by turbulent kinetic energy (TKE) dissipation, which is a missing physics term in the GFS model, is parameterized and included in the hybrid EDMF PBL scheme. With the inclusion of TKE dissipative heating, a large atmospheric energy loss in the GFS atmosphere–ocean coupled run is largely reduced and the hurricane intensity is significantly increased in the GFS forecast. To enhance the vertical turbulent mixing that is too weak in the case of a stable boundary layer (SBL), the current local scheme is modified to use an ED profile method for weakly and moderately stable conditions with varying critical bulk Richardson numbers for determining the PBL height.

Medium-range forecasts have been conducted to assess the impacts on forecast skill of the new hybrid EDMF PBL scheme with the TKE dissipative heating and the modifications in the SBL mixing scheme. The new scheme presents a significant improvement for the 500-hPa height anomaly correlations, which is one of the most important forecast skill measurements since it illustrates how well synoptic-scale systems are represented around the globe. For precipitation forecasts over the continental United States and hurricane forecasts, the new scheme shows a neutral skill. The hybrid EDMF PBL scheme with TKE dissipative heating and modification in the SBL was operationally implemented in the January 2015 NCEP GFS upgrade as tests with this scheme showed a positive impact on the GFS medium-range forecasts.

This study is a first step toward including an EDMF parameterization of the PBL in the GFS. For further improvement of the EDMF parameterization, we are currently developing an EDMF scheme based on a TKE closure model that requires a prognostic equation for TKE. With the memory of turbulence retained, the TKE-based EDMF scheme may better handle vertical turbulent mixing, especially for a PBL with weak turbulence, which in turn, may help to improve model performance for weakly unstable conditions over the tropical ocean. A unified EDMF model of PBL and shallow convection is also under development.

Acknowledgments. This work was supported by the NOAA MAPP/CPO program as part of the Sc-to-Cu Transition Climate Process Team. Internal reviews from Helin Wei, Qingfu Liu, and Mary Hart at NCEP/EMC are highly appreciated. We also thank the anonymous reviewers for valuable comments that helped to improve the manuscript.

REFERENCES

Bister, M., and K. A. Emanuel, 1998: Dissipative heating and hurricane intensity. *Meteor. Atmos. Phys.*, **65**, 233–240, doi:10.1007/BF01030791.

Brown, A. R., and A. L. M. Grant, 1997: Non-local mixing of momentum in the convective boundary layer. *Bound.-Layer Meteor.*, **84**, 1–12, doi:10.1023/A:1000388830859.

Clough, S. A., M. W. Shephard, E. J. Mlawer, J. S. Delamere, M. J. Iacono, K. Cady-Pereira, S. Boukabara, and P. D. Brown, 2005: Atmospheric radiative transfer modeling: A summary of the AER codes. *J. Quant. Spectrosc. Radiat. Transfer*, **91**, 233–244, doi:10.1016/j.jqsrt.2004.05.058.

Cuxart, J., and Coauthors, 2006: Single-column model intercomparison for a stably stratified atmospheric boundary layer. *Bound.-Layer Meteor.*, **118**, 273–303, doi:10.1007/s10546-005-3780-1.

Deardorff, J. W., 1966: The counter-gradient heat flux in the lower atmosphere and in the laboratory. *J. Atmos. Sci.*, **23**, 503–506, doi:10.1175/1520-0469(1966)023<0503:TCGHFI>2.0.CO;2.

de Roode, S. R., A. P. Siebesma, H. J. J. Jonker, and Y. de Voogd, 2012: Parameterization of the vertical velocity equation for shallow cumulus clouds. *Mon. Wea. Rev.*, **140**, 2424–2436, doi:10.1175/MWR-D-11-00277.1.

Ek, M. B., K. E. Mitchell, Y. Lin, E. Rogers, P. Grummann, V. Koren, G. Gayno, and J. D. Tarplay, 2003: Implementation of the Noah land-use model advances in the NCEP operational mesoscale Eta Model. *J. Geophys. Res.*, **108**, 8851, doi:10.1029/2002JD003296.

Fiedler, B. H., 2000: Dissipative heating in climate models. *Quart. J. Roy. Meteor. Soc.*, **126**, 925–939, doi:10.1002/qj.49712656408.

Frech, M., and L. Mahrt, 1995: A two-scale mixing formulation for the atmospheric boundary layer. *Bound.-Layer Meteor.*, **73**, 91–104, doi:10.1007/BF00708931.

Gandin, L. S., and A. H. Murphy, 1992: Equitable skill scores for categorical forecasts. *Mon. Wea. Rev.*, **120**, 361–370, doi:10.1175/1520-0493(1992)120<0361:ESSFCF>2.0.CO;2.

Han, J., and H.-L. Pan, 2006: Sensitivity of hurricane intensity forecast to convective momentum transport parameterization. *Mon. Wea. Rev.*, **134**, 664–674, doi:10.1175/MWR3090.1.

——, and ——, 2011: Revision of convection and vertical diffusion schemes in the NCEP Global Forecast System. *Wea. Forecasting*, **26**, 520–533, doi:10.1175/WAF-D-10-05038.1.

Hong, S.-Y., 2010: A new stable boundary-layer mixing scheme and its impact on the simulated East Asian summer monsoon. *Quart. J. Roy. Meteor. Soc.*, **136**, 1481–1496, doi:10.1002/qj.665.

——, and H.-L. Pan, 1996: Nonlocal boundary layer vertical diffusion in a medium-range forecast model. *Mon. Wea. Rev.*, **124**, 2322–2339, doi:10.1175/1520-0493(1996)124<2322:NBLVDI>2.0.CO;2.

Hourdin, F., and Coauthors, 2013: LMDZ5B: The atmospheric component of the IPSL climate model with revisited parameterizations for clouds and convection. *Climate Dyn.*, **40**, 2193–2222, doi:10.1007/s00382-012-1343-y.

Iacono, M. J., E. J. Mlawer, S. A. Clough, and J.-J. Morcrette, 2000: Impact of an improved longwave radiation model, RRTM, on the energy budget and thermodynamic properties of the NCAR Community Climate Model, CCM3. *J. Geophys. Res.*, **105**, 14 873–14 890, doi:10.1029/2000JD900091.

Jin, Y., W. T. Thompson, S. Wang, and C.-S. Liou, 2007: A numerical study of the effect of dissipative heating on tropical cyclone intensity. *Wea. Forecasting*, **22**, 950–966, doi:10.1175/WAF1028.1.

Khairoutdinov, M. F., and D. A. Randall, 2003: Cloud resolving modeling of the ARM summer 1997 IOP: Model formulation, results, uncertainties, and sensitivities. *J. Atmos. Sci.*, **60**, 607–625, doi:10.1175/1520-0469(2003)060<0607:CRMOTA>2.0.CO;2.

Kim, Y.-J., and A. Arakawa, 1995: Improvement of orographic gravity wave parameterization using a mesoscale gravity wave model. *J. Atmos. Sci.*, **52**, 1875–1902, doi:10.1175/1520-0469(1995)052<1875:IOOGWP>2.0.CO;2.

Köhler, M., M. Ahlgrimm, and A. Beljaars, 2011: Unified treatment of dry convective and stratocumulus-topped boundary layers in the ECMWF model. *Quart. J. Roy. Meteor. Soc.*, **137**, 43–57, doi:10.1002/qj.713.

Long, P. E., 1986: An economical and compatible scheme for parameterizing the stable surface layer in the medium range forecast model. NCEP Office Note 321, 24 pp. [Available online at http://www.lib.ncep.noaa.gov/ncepofficenotes/files/01408602.pdf.]

——, 1989: Derivation and suggested method of the application of simplified relations for surface fluxes in the medium-range forecast model: Unstable case. NCEP Office Note 356, 53 pp. [Available online at http://www.lib.ncep.noaa.gov/ncepofficenotes/files/0140893E.pdf.]

Mlawer, E. J., S. J. Taubman, P. D. Brown, M. J. Iacono, and S. A. Clough, 1997: RRTM, a validated correlated-*k* model for the longwave. *J. Geophys. Res.*, **102**, 16 663–16 682, doi:10.1029/97JD00237.

Moorthi, S., H.-L. Pan, and P. Caplan, 2001: Changes to the 2001 NCEP operational MRF/AVN global analysis/forecast system. NWS Tech. Procedures Bull. 484, 14 pp. [Available online at http://www.nws.noaa.gov/om/tpb/484.pdf.]

Neggers, R. A. J., A. P. Siebesma, and H. J. J. Jonker, 2002: A multiparcel model for shallow cumulus convection. *J. Atmos. Sci.*, **59**, 1655–1668, doi:10.1175/1520-0469(2002)059<1655:AMMFSC>2.0.CO;2.

——, M. Köhler, and A. C. M. Beljaars, 2009: A dual mass flux framework for boundary layer convection. Part I: Transport. *J. Atmos. Sci.*, **66**, 1465–1487, doi:10.1175/2008JAS2635.1.

Noh, Y., W. G. Cheon, S.-Y. Hong, and S. Raasch, 2003: Improvement of the profile model for the planetary boundary layer based on large eddy simulation data. *Bound.-Layer Meteor.*, **107**, 401–427, doi:10.1023/A:1022146015946.

Park, B.-K., and S.-Y. Hong, 2013: Effects of physics packages on medium-range forecasts in a global forecasting system. *J. Atmos. Sol.-Terr. Phys.*, **100–101**, 50–58, doi:10.1016/j.jastp.2013.03.027.

Rio, C., and F. Hourdin, 2008: A thermal plume model for the convective boundary layer: Representation of cumulus clouds. *J. Atmos. Sci.*, **65**, 407–425, doi:10.1175/2007JAS2256.1.

Siebesma, A. P., and J. Teixeira, 2000: An advection–diffusion scheme for the convective boundary layer: Description and 1d-results. Preprints, *14th Symp. on Boundary Layers and Turbulence,* Aspen, CO, Amer. Meteor. Soc., 133–136.

——, P. M. M. Soares, and J. Teixeira, 2007: A combined eddy-diffusivity mass-flux approach for the convective boundary layer. *J. Atmos. Sci.*, **64**, 1230–1248, doi:10.1175/JAS3888.1.

Soares, P. M. M., P. M. A. Miranda, A. P. Siebesma, and J. Teixeira, 2004: An eddy-diffusivity/mass-flux parameterization for dry and shallow cumulus convection. *Quart. J. Roy. Meteor. Soc.*, **130**, 3365–3384, doi:10.1256/qj.03.223.

Sorbjan, Z., 1989: *Structure of the Atmospheric Boundary Layer.* Prentice Hall, 317 pp.

Sundqvist, H., E. Berge, and J. E. Kristjansson, 1989: Condensation and cloud studies with mesoscale numerical weather prediction model. *Mon. Wea. Rev.*, **117**, 1641–1657, doi:10.1175/1520-0493(1989)117<1641:CACPSW>2.0.CO;2.

Sušelj, K., T. F. Hogan, and J. Teixeira, 2014: Implementation of a stochastic eddy-diffusivity/mass-flux parameterization into the Navy Global Environmental Model. *Wea. Forecasting*, **29**, 1374–1390, doi:10.1175/WAF-D-14-00043.1.

Troen, I. B., and L. Mahrt, 1986: A simple model of the atmospheric boundary layer sensitivity to surface evaporation. *Bound.-Layer Meteor.*, **37**, 129–148, doi:10.1007/BF00122760.

Vickers, D., and L. Mahrt, 2004: Evaluating formulations of stable boundary layer height. *J. Appl. Meteor.*, **43**, 1736–1749, doi:10.1175/JAM2160.1.

Witek, M. L., J. Teixeira, and G. Matheou, 2011: An integrated TKE-based eddy-diffusivity/mass-flux boundary layer closure for the dry convective boundary layer. *J. Atmos. Sci.*, **68**, 1526–1540, doi:10.1175/2011JAS3548.1.

Xu, K.-M., and D. A. Randall, 1996: A semiempirical cloudiness parameterization for use in climate models. *J. Atmos. Sci.*, **53**, 3084–3102, doi:10.1175/1520-0469(1996)053<3084:ASCPFU>2.0.CO;2.

Zhang, D.-L., and E. Altshuler, 1999: The effects of dissipative heating on hurricane intensity. *Mon. Wea. Rev.*, **127**, 3032–3038, doi:10.1175/1520-0493(1999)127<3032:TEODHO>2.0.CO;2.

Zhang, G. J., and X. Wu, 2003: Convective momentum transport and perturbation pressure field from a cloud-resolving model simulation. *J. Atmos. Sci.*, **60**, 1120–1139, doi:10.1175/1520-0469(2003)060<1120:CMTAPP>2.0.CO;2.

Zhao, Q., and F. H. Carr, 1997: A prognostic cloud scheme for operational NWP models. *Mon. Wea. Rev.*, **125**, 1931–1953, doi:10.1175/1520-0493(1997)125<1931:APCSFO>2.0.CO;2.